Hydrological Sciences – Journal – des Sciences Hydrologiques, 32, 3, 9/1987

Macroscale analysis of upland erosion

PIERRE Y. JULIEN
Department of Civil Engineering, Colorado State University, Fort Collins, Colorado 80523, USA

MARCEL FRENETTE
Department of Civil Engineering, Laval University, Quebec, Canada G1K 7P4

ABSTRACT Scale effects in computing sheet and rill erosion losses from large basins have been studied for grid sizes ranging from 0.03 to 4 km^2 over drainage areas up to 3000 km^2. As a result of the analysis conducted on the Chaudière basin (5830 km^2), the mean characteristics of the basin can be used to estimate the mean annual upland erosion losses after a correction factor for the influence of grid size is introduced into the calculation. The use of fine-meshed grids can be justified when information on the areal distribution of soil erosion is desired.

Analyse macroscopique de l'érosion superficielles
RESUME Une méthode de prédétermination d'érosion superficielle sur les grands bassins versants a été mise au point à partir d'une étude détaillée du bassin de la rivière Chaudière (A = 5830 km^2). Plusieurs grilles dont la taille varie de 0.03 à 4 km^2 ont été superposées au bassin pour calculer l'érosion pluviale sur des superficies atteignant 3000 km^2. Un facteur de correction fonction de la superficie drainée est introduit dans les équations. Il en résulte que l'érosion totale des grands bassins est estimée à partir des caractéristiques moyennes du bassin. L'utilisation de quadrillages devient justifiable pour définir la distribution spatiale de l'érosion superficielle.

NOTATION

A_o	drainage area of cells
A	drainage area
C	area-weighted value of the crop management factor
C_o	crop management factor
C_v	coefficient of variation for the sum of erosion losses from N independent units
e	estimate of the annual soil erosion loss per unit area
e_o	annual soil erosion loss per unit area
h_1	minimum elevation on an infinitesimal unit
h_2	maximum elevation on an infinitesimal unit
h_{max}	maximum elevation on one unit

Open for discussion until 1 March 1988.

h_{min}	minimum elevation on one unit
ℓ	size of a grid
N	number of units
Q_e	correction factor for the grid size
$\bar{Q}_e$	mean value of the correction factor
Q_e^*	relative correction factor
$\bar{Q}_{es}$	expected value of the correction factor for small grid sizes
$\bar{Q}_e^*$	mean value of the relative correction factor
Q_{e95}	confidence interval at 95 percent of the correction factor
S_o	slope on infinitesimal grids
S	slope estimator
β	exponent of slope in the soil loss equation
θ	angle between contour lines and the side of infinitesimal grid sizes
σ	standard deviation of log-transformed correction factors
σ_s	standard deviation of the sum of N independent log-transformed correction factors

INTRODUCTION

Rainfall-induced overland flow has the ability to detach and transport large amounts of sediment from upland areas. Sheet and rill erosion losses are complex processes related to landform geometry, surface slope, overland runoff length, rainfall intensity, soil infiltration rate, interception, storage, ground cover, canopy cover, evaporation, evapotranspiration, land use and conservation practices. The fundamentals of soil erosion and conservation are detailed in Hudson (1981), Zachar (1982), Jansson (1981), and Schwab *et al.* (1981). Methodologies to quantify erosion losses include the widely used Universal Soil-Loss Equation (USLE) which has been derived for data from small experimental plots.

Because soil-loss equations were developed for small upland areas (about one hectare), small basins are preferably discretized into small homogeneous areas to evaluate soil erosion losses from the drainage area. Square grids can be superimposed onto drainage basins with the mesh size conditioned by the applicability of the soil-loss equation. This method has been successfully applied to drainage areas up to 50 km^2 and soil erosion maps can be plotted with the aid of computers. The inherent limitations of this method are the data requirements which become prohibitive as the size of the drainage area increases beyond 100 km^2.

It seems interesting to examine whether larger grid sizes beyond the limit of applicability of soil-loss equations could provide sufficient accuracy in predicting upland erosion losses. The investigation reported here discusses the applicability of upland erosion equations to large drainage areas. Detailed information from the Chaudière basin in Canada is scrutinized to determine the scale effects associated with various grid sizes in the calculation of soil erosion losses. The development of simple methodologies to estimate on-site erosion losses over large basins with minimum data requirements also figures among the research objectives of foremost importance.

FIELD SITE AND DATA SOURCES

The Chaudière basin shown in Fig.1 was selected for this study. This Appalachian basin covers an area of 5830 km^2 to St-Lambert-de-Lévis where the downstream gauging station is located.

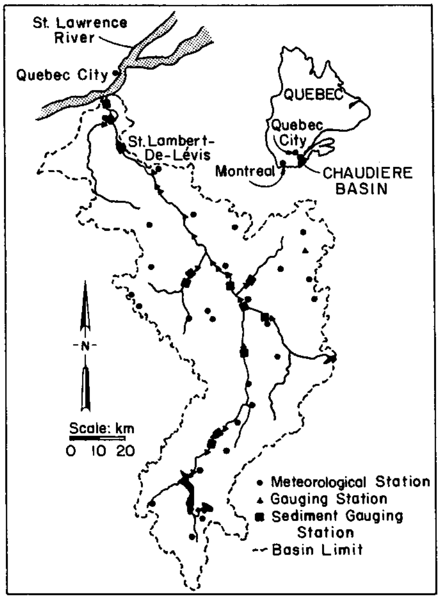

Fig. 1 Location of the Chaudière basin.

The basin geometry, vegetation and land use were accurately determined from topographical maps (1:50 000), land use and soil classification maps (1:200 000), forest maps (1:125 000), aerial photographs and Landsat imagery. Data from a network of 22 meteorological stations, 16 gauging stations and nine sediment gauging stations were available on a daily basis. Approximately 65% of the basin is still forested whereas 35% is used for agriculture and pasture lands. All the parameters related to soil erosion have been carefully documented (Julien, 1979, 1982; Frenette & Julien, 1986). Data analysis shows a relative uniformity of rainfall erosivity, soil erodibility and conservation practice on the drainage basin.

The annual soil erosion loss per unit area, e_o, in kt km^{-2} is a function of the slope, S_o, in m m^{-1} and the crop-management factor, C_o, of the USLE. For the Chaudière basin the following relationship is applicable for predicting rainfall erosion losses:

$$e_o = 226 \, S_o^{\beta} \, C_o \quad (1)$$

Detailed investigations (Julien, 1979; Julien & Frenette, 1986a) showed that the results obtained with Kilinc and Richardson's method (β = 1.46) are in close agreement with those of the USLE. Julien & Simons (1985) showed similarities between several sediment transport relationships for overland flow, including the USLE, and the values of the exponent, β, using different methods are given.

GRID SIZE ANALYSIS

When an infinitesimal square grid is superimposed onto the drainage basin, the slope and crop-management factors become uniform for each unit. The actual slope, S_o, in m m^{-1} on the unit is calculated from the minimum and maximum elevations h_1 and h_2, located on opposite corners of a square unit of size, ℓ, and angle, θ, sketched in Fig.2:

$$S_o = \frac{h_2 - h_1}{\ell(\cos\theta + \sin\theta)} \tag{2}$$

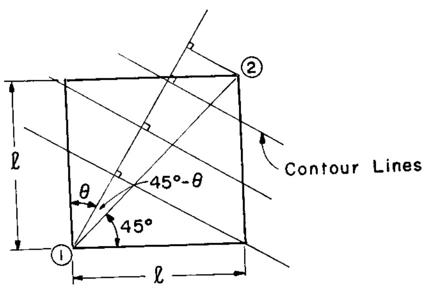

Fig. 2 Infinitesimal grid.

With increasing grid size, the slope varies within each unit and the extreme elevations are not found on opposite corners. The following estimate of slope, S, in m m^{-1} is defined as a function of the maximum elevation h_{max}, in m, the minimum elevation, h_{min}, in m, and the drainage area, A, in m^2:

$$S = \frac{h_{max} - h_{min}}{\sqrt{A}} \tag{3}$$

Similarly, the area-weighted value of the crop management factor, C, is employed for large areas. Substituting S and C for S_o and C_o in equation (1) yields the soil loss estimator, e. The ratio, e/e_o, defines the correction factor, Q_e, which is to be used with the soil loss estimator, e, to determine the actual erosion losses, e_o.

For infinitesimal grids, equations (1), (2) and (3) yield the following relationship for Q_e as a function of θ and β, given that $C = C_o$, and $A = \ell^2$:

$$Q_e = (\cos\theta + \sin\theta)^{\beta} \qquad (4)$$

The gradual increase in Q_e with θ and β is illustrated in Fig.3(a). Obviously Q_e reduces to unity when $\beta = 0$, or when $\theta = 0$.

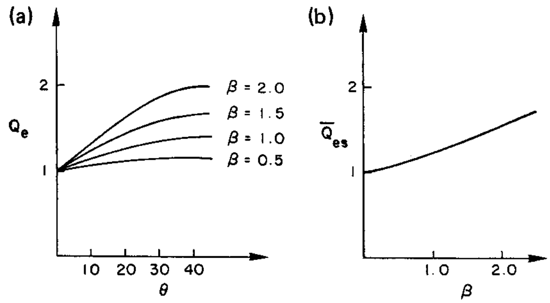

Fig. 3 (a) Variation of Q_e with θ and β for infinitesimal grids; (b) expected value of the correction factor, $\bar{Q}_{es}$, for infinitesimal grids.

When the angle, θ, is unknown, the following procedure has been developed. Considering the random variability of the angle θ, the analytical expression of the expected value of the correction factor, $\bar{Q}_{es}$, is:

$$\frac{1}{\bar{Q}_{es}} = \frac{4}{\pi} \int_0^{\pi/4} \frac{d\theta}{(\cos\theta + \sin\theta)^{\beta}} \qquad (5)$$

The results of the numerical integration of equation (5), plotted in Fig.3(b), indicate a gradual increase in $\bar{Q}_{es}$ with β.

For larger drainage areas, the following grid size analysis has been conducted. Square areas were randomly selected from the Chaudière basin as shown in Fig.4. The square areas were subdivided into matrices of 12 x 12 cells and classified in Table 1 into three sets according to the area of the cells. The surface area of cells in Data Sets A, B and C is respectively 2.8 ha, 25 ha and 4 km^2. In addition, Data Set D combines 4 km^2 cells into large square matrices with surface areas ranging from 4 to 3000 km^2 over the entire basin.

For each of the areas of the four Data Sets, a relative correction factor, Q_e^* (an asterisk is used to denote relative correction factors), has been defined as the ratio of soil erosion from the total area, A, over the sum of individual losses from each cell; this is schematized in Fig.5 for a small 2 x 2 matrix. The calculation procedure is repeated for larger matrices (3 x 3; 4 x 4; 6 x 6...) and details of the computerized data analysis are presented in Julien (1979).

Several thousand values of the relative correction factor were computed; Q_e^* depends on the number of cells, N, and the size A_o, of the cells. For given values of A_o and N, the first three moments

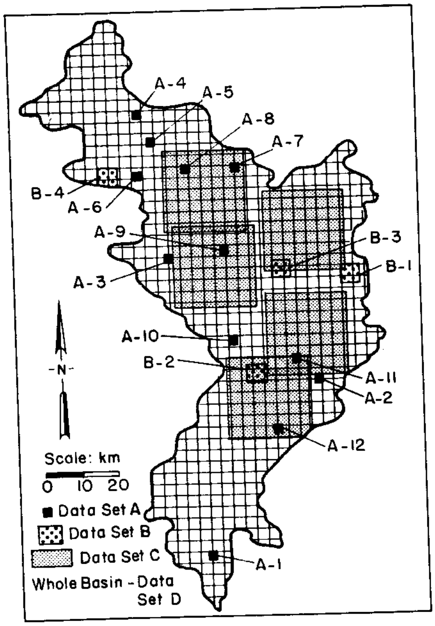

Fig. 4 Random selection of square areas for the grid size analysis.

Table 1 Scope of grid size analysis

Data Set	Cell area (km^2)	Matrix size	Matrix area (km^2)	Number of matrices
A	0.028	144 (12 x 12)	4	12
B	0.25	144 (12 x 12)	36	4
C	4.0	144 (12 x 12)	576	5
D	4.0	up to 1600	3000	N/A

N/A Not Applicable.

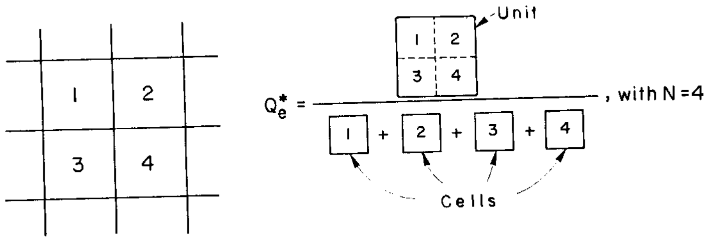

Fig. 5 Definition sketch for the relative correction factor, Q_e^*.

of the distribution of log Q_e^* give very low values of the skewness coefficient. Therefore, it was hypothesized and verified that Q_e^* is lognormally distributed; the results of the analysis for Data Set B are shown in Fig.6 as an example. The mean value and the confidence intervals at 95% are obtained from the following analysis of the first two moments.

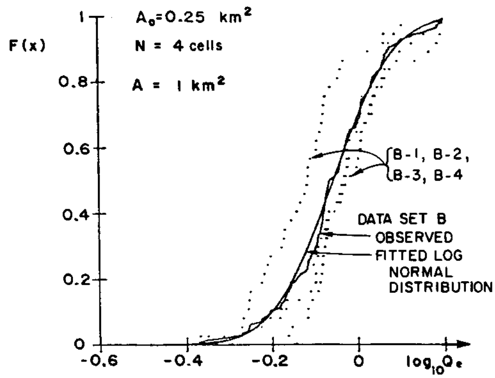

Fig. 6 Observed and fitted distribution function of Q_e for the Data Set B.

Mean value of the correction factor

The mean value of the log-transformed relative correction factor, $\bar{Q}_e^*$, shown in Fig.7 gradually decreases as N increases for all sets. The only exception to this general trend is that values of $\bar{Q}_e^*$ remain constant for $N < 9$ on the smallest drainage areas (Data Set A). Interestingly, this corresponds to the expected correction factor, $\bar{Q}_{es}$, discussed previously (Fig.3(b)). The value of $\bar{Q}_{es} = 1.13$ has been obtained for drainage areas smaller than 0.125 km^2 on the Chaudière basin when the USLE was used for the calculation of soil erosion. For larger areas, regression analysis gives the following relative correction factor, $\bar{Q}_e^*$, as a function of $\bar{Q}_{es}$, A and A_o:

$$\log \bar{Q}_e^* = +0.0061 - 0.137 \log A + 0.083 \log A_o \quad (6)$$

A correction factor, $\bar{Q}_e$, is defined by the following change of variables:

$$\log \bar{Q}_e = \log \bar{Q}_e^* - 0.083 \log A_o - 0.129 + \log \bar{Q}_{es} \quad (7)$$

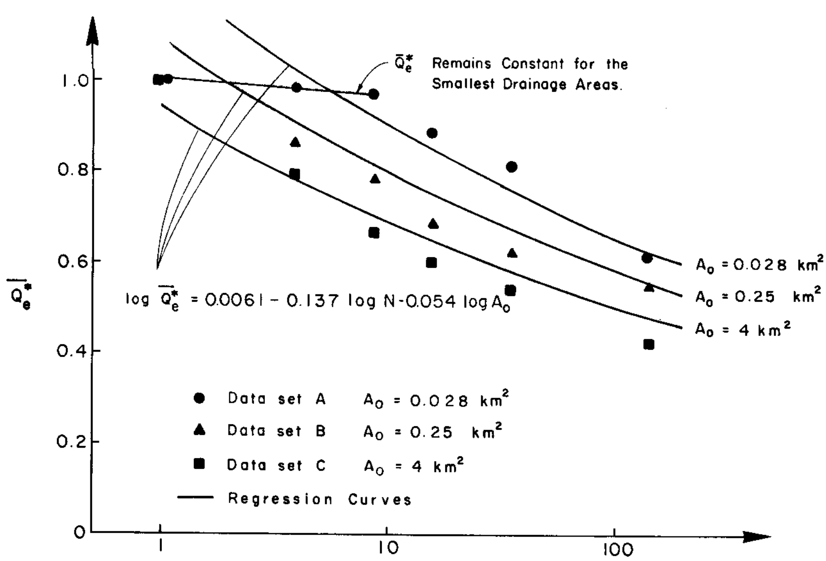

Fig. 7 Mean value of log $\bar{Q}_e^*$ *vs.* the number of cells, N.

Thus substituting equation (7) into equation (6), the correction factor, $\bar{Q}_e$, becomes independent of A_o with the following relationship:

$$\bar{Q}_e = 0.75\ \bar{Q}_{es} A^{-0.137} \qquad A > 0.125\ km^2 \tag{8}$$

As a result, with $\bar{Q}_{es} = 1.13$, a correction factor, $\bar{Q}_e$, which is a function of the drainage area only is obtained and all the data from Fig.6 collapse onto a single curve shown in Fig.8. Two governing laws for the correction factor, $\bar{Q}_e$, are identified. First, for $A < 0.125\ km^2$, the correction factor, $\bar{Q}_e$, remains constant ($\bar{Q}_e = \bar{Q}_{es}$) which indicates that the soil loss equation can be applied to these areas without bias. As the drainage area increases beyond the threshold value $A > 0.125\ km^2$, the correction factor, $\bar{Q}_e$, decreases gradually as shown in Fig.8.

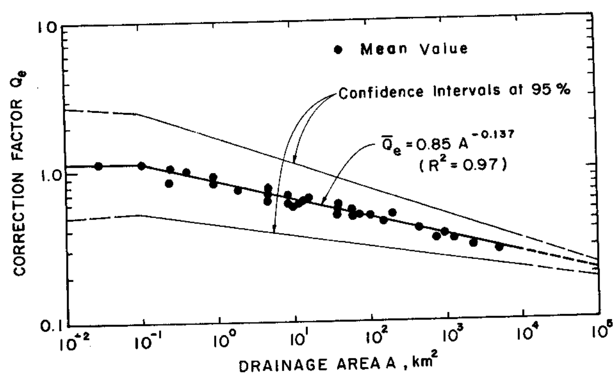

Fig. 8 Mean value and confidence intervals at 95% of the correction factor, Q_e, *vs.* drainage area, A.

Confidence intervals of the correction factor

The standard deviations, σ, of the log-transformed relative correction factor, Q_e^*, for Data Sets A, B and C are shown in Fig.9. All three Data Sets have similar shapes with an increase in σ for $N < 9$, a peak around $9 < N < 36$ and then a gradual decrease for $N > 36$. As a second interesting feature, the magnitude of the peak decreases as A_o increases. Regression analysis provides a quantitative relationship for the standard deviation, σ. After substituting A_o with A/N, the following regression relationship has been obtained.

$$\sigma = 0.00235 + \left[\frac{N-1}{N}\right] (0.148 - 0.0226 \log A) \tag{9}$$

Note that under this form the standard deviation, σ, depends on the drainage area, A, and the number of cells, N. The standard deviation decreases to zero as N approaches unity. As N increases, the term in brackets reduces to unity and σ becomes solely a function of A.

The confidence intervals of the correction factor, Q_e, are

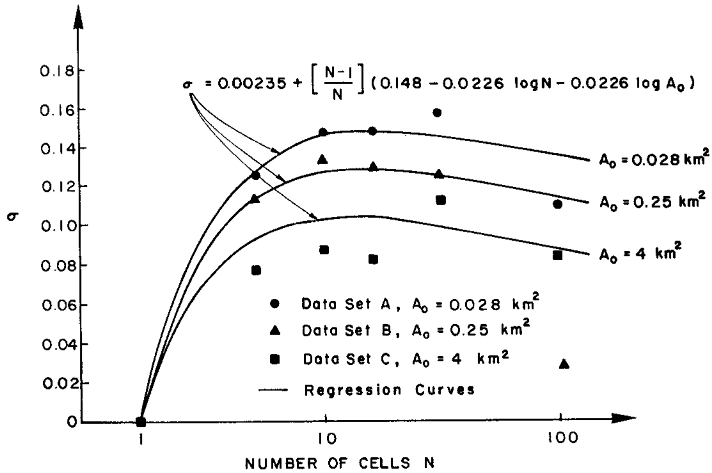

Fig. 9 Standard deviation, σ, of $\log \bar{Q}_e^*$ *vs.* the number of cells, N.

obtained after combining equations (8) and (9) using the properties of lognormal distributions for Q_e. The confidence interval at 95% can be written:

$$Q_{e95} = \bar{Q}_e \times 10^{\pm 1.96\sigma} \tag{10}$$

Agreement between equation (10) and the Data Set D is shown in Fig.10. Confidence intervals at 66% are given after replacing 1.96 in equation (10) with unity. As N becomes large, the expression for the confidence intervals reduces to a function of Q_e and A which has been plotted in Fig.8. These results can be used for design purposes as discussed below.

The foremost conclusion of this analysis is drawn from the

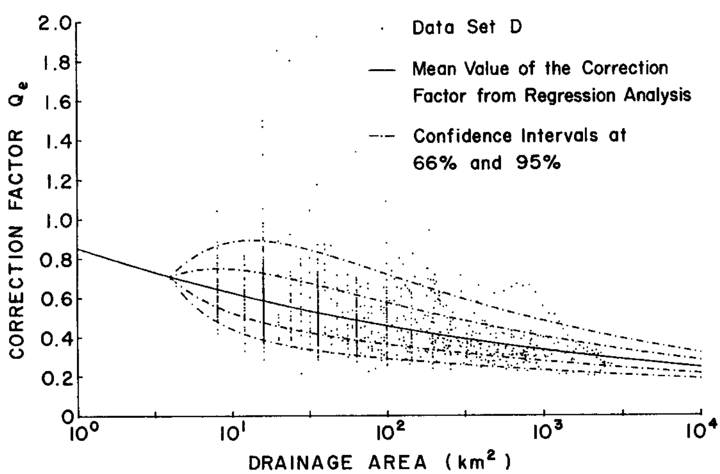

Fig. 10 Mean value and confidence intervals at 66% and 95% of the correction factor, Q_e, for Data Set D.

gradual decrease of the standard deviation with increase in drainage area. This property enables the development of a reasonably accurate method to estimate the total upland erosion losses for large drainage basins. Indeed the results shown in Fig.8 indicate that for drainage basins as large as 1000 km^2, the variability of the correction factor ranged from 0.17 to 0.49 (from equation (10)) with a mean value of 0.33 (from equation (8)). Therefore, a first estimate of the total annual upland erosion losses can be obtained from the soil loss estimator, e, and the average correction factor, $\bar{Q}_e$. Examples are given in Frenette & Julien (1980) and Julien & Frenette (1986b).

When the erosion loss from a large basin is calculated from the sum of N independent calculation units, the standard deviation of the sum, σ_s, is obtained after considering the lognormal distribution of the log-transformed correction factors, thus:

$$\sigma_s = \frac{\sigma}{\sqrt{N}} \tag{11}$$

As could be expected, σ_s decreases as the number of calculation units, N, increases. The coefficient of variation, C_v, of the sum is therefore given by:

$$C_v = 10^{\sigma_s} - 1 \tag{12}$$

After combining equations (9), (11), and (12), the coefficient of variation is illustrated in Fig.11 as a function of A and N. For example, when a drainage basin covering an area of *1000* km^2 is subdivided into N = 1000 units for the calculation of soil erosion, the coefficient of variation of the sum (Fig.11) is less than 1%, as compared to C_v = 6% when the same drainage area is subdivided into N = 10 units.

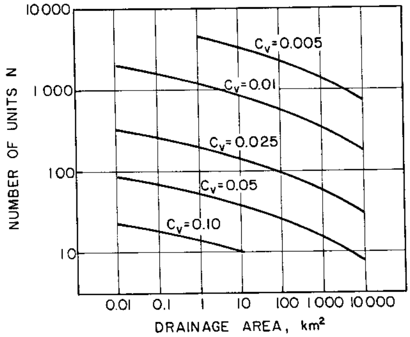

Fig. 11 Coefficient of variation of the sum of N independent upland erosion losses.

This conclusion remains valid when a large number of independent units from the same population is considered. The validity of the method depends mostly on the applicability of the sediment transport relationship, equation (1). The method should preferably be used on morphologically homogeneous basins since the same soil loss equation is applied to the entire watershed.

CONCLUSION

A substantial analysis of the influence of grid size in calculating sheet and rill erosion losses from upland areas has been presented. Using grid sizes ranging from 0.03 to 3000 km^2 in the Chaudière basin, a correction factor, Q_e, which is a function of the grid size, has been defined and shown in Fig.8. The mean value of Q_e and the confidence intervals at 95% decrease gradually when $A > 0.125\ km^2$. A simplified method has been developed to provide estimates of the total soil erosion losses from the mean characteristics of a large drainage basin. Fine-meshed grids are best used to define the spatial distribution of soil erosion, and for better accuracy in predicting the total upland erosion losses from large basins. Quantitative evaluation can be made from Fig.11 as a function of drainage area and number of units.

ACKNOWLEDGEMENTS This study has been carried out at Laval University, Canada. The support from the Civil Engineering Department and the CTI at Laval University for conducting computerized research is gratefully acknowledged.

REFERENCES

Frenette, M. & Julien, P.Y. (1980) Méthode simplifiée de prédiction d'érosion de bassin versant et d'apport solide en suspension dans les cours d'eau nordiques. *Proc. Second Hydrotechnical Conference* (CSCE-Quebec, Sherbrooke, Canada).

Frenette, M. & Julien, P.Y. (1986) LAVSED I - Un modèle pour prédire l'érosion des bassins et le transfert des sédiments fins dans les cours d'eau nordiques. *Can. J. Civ. Engng*, CSCE 13(2), 150-161.

Hudson, N. (1981) *Soil Conservation*. Cornell Univ., Ithaca, New York, USA.

Jansson, M. (1981) Land erosion by water in different climates. *UNGI Report 57, Uppsala Univ.*

Julien, P. (1979) Erosion de bassin et apport solide en suspension dans les cours d'eau nordiques. MS Thesis, Laval Univ., Québec, Canada.

Julien, P. (1982) Prédiction d'apport solide pluvial et nival dans les cours d'eau nordiques à partir du ruissellement superficiel. PhD Dissertation, Laval Univ., Québec, Canada.

Julien, P.Y. & Frenette, M. (1986a) LAVSEDII - A model for predicting soil erosion and washload in streams. *Can. J. Civ. Engng*, CSCE 13(2), 162-170.

Julien, P.Y. & Frenette, M. (1986b) Scale effects in predicting soil erosion. In: *Drainage Basin Sediment Delivery* (Proc.

Albuquerque Symp., August 1986), 253-259. IAHS Publ.no.159.
Julien, P.Y. & Simons, D.B. (1985) Sediment transport capacity of overland flow. *Trans Am. Soc. Agric. Engrs* 28(3), 755-762.
Kilinc, M. & Richardson, E.V. (1973) Mechanics of Soil Erosion from Overland Flow Generated by Simulated Rainfall. *Hydrol. Pap. 63, Colorado State University, Fort Collins, Colorado.*
Schwab, G.O., Frevert, R.K., Edminster, T.W. & Barnes, K.K. (1981) *Soil and Water Conservation Engineering.* Wiley, Chichester, UK.
Zachar, D. (1982) *Soil Erosion.* Developments in Soil Science 10, Elsevier.

Received 1 October 1986; accepted 25 February 1987.